Eur. Phys. J. Special Topics **228**, 2233–2245 (2019)
© EDP Sciences, Springer-Verlag GmbH Germany, part of Springer Nature, 2019
https://doi.org/10.1140/epjst/e2019-900040-x

THE EUROPEAN PHYSICAL JOURNAL SPECIAL TOPICS

Regular Article

A new chaotic oscillator containing generalised memristor, single op-amp and RLC with chaos suppression and an application for the random number generation

Jay Prakash Singh[1,3,a], Jit Koley[3], Akif Akgul[2], Bilal Gurevin[2], and Binoy Krishna Roy[3]

[1] Department of Electrical Engineering, Rewa Engineering College, Rewa 486602, MP, India
[2] Department of Electrical and Electronic Engineering, Faculty of Technology, Sakarya University of Applied Sciences, Serdivan, Turkey
[3] Department of Electrical Engineering, National Institute of Technology Silchar, Silchar 788010 Assam, India

Received 15 February 2019 / Received in final form 7 May 2019
Published online 14 October 2019

Abstract. In this paper, a new chaotic oscillator consists of a single op-amp, two capacitors, one resistor, one inductor, and memristive diode bridge cascaded with an inductor is proposed. The proposed chaotic oscillator has a line of equilibria. In the new oscillator circuit, negative feedback, i.e. inverting terminal of the op-amp is used, and the non-inverting terminal is grounded. The new oscillator has chaotic, periodic, quasi-periodic behaviours, as seen from the Lyapunov spectrum plots. Some more theoretical and numerical tools are used to present the dynamical behaviours of the new oscillator like bifurcation diagram, phase plot. Further, a non-singular terminal sliding mode control (N-TSMC) is designed for the suppression of the chaotic states of the new oscillator. An application of the new oscillator is shown by designing a chaos-based random number generator. Raspberry Pi 3 is used for the realisation of the random number generator.

1 Introduction

In the present decade, analogue components with memory are more focused on the research [1,2]. Initial works on memristor were reported in [3–5]. The circuit components with memory are considered as memristor, meminductor and memcapacitor [1]. The behaviour of these components is dependent on their history. The physical realisation of a memristor was only done by HP laboratory [4], and not commercially available now. Besides this challenge, the circuit elements with memory are more interesting.

The nonlinear characteristics of a memristor make it more attractive to use in chaotic circuits. Moreover, the analysis, design, development and application of a memristor have become a recent trend in research. Sometimes, the number of the state

[a] e-mail: jayprakash1261@gmail.com

Table 1. Categorisation of research on the single op-amp based chaotic oscillators.

Sl. No.	Category/classification	References
1.	1-opamp, 3-R, 1-C and voltage-controlled voltage source	[29]
2.	1-opamp, 4-R, 2-C and parallel diode-inductor	[16,17]
3.	1-opamp, 4-R, 2-C and parallel Diode- Antoniou General Impedance Converter (GIC) arrangement	[19]
4.	1-opamp, 5-R, 3-C and 1-Chua's diode	[30]
5.	1-opamp, 1-R, 2-C, 1-L, 1-Diode	[26]
6.	Wein-bridge oscillators: 1-opamp, 5-R, 2-C, diodes/Chua's diode	[6,20]
7.	Wien-bridge oscillator: non-autonomous	[31]
8.	1-opamp, 1-R, 1-L, 2-C and pair of semiconductor diodes memristor-based	[27]
9.	Wein-bridge oscillators: different types of memristor, 1-opamp and Rs, Cs	[18,21–25,28]
10.	1-opamp, 2-C, 1-R, 1-L, and memristive diode bridge cascaded with an inductor	This work

equations increases significantly for a memory-based chaotic circuit that enhances the difficulty level for its analysis and solution [6]. There are many research directions available for the use of a memristor in a chaotic circuit [7–11]. Some of these circuits are like non-smooth piecewise-linear [12], curve model [8,11], piecewise quadric non-linearity [13], memristor-based neural network [14], etc. Despite these, the research on the use of a memristor in a chaotic circuit has been comparatively less explored as compared with the use of normal chaotic circuits.

It has always being focused to develop a simple chaotic oscillator compared with the available one. A simple chaotic oscillator is required for reporting a new system since a new chaotic system must satisfy at least one criterion in [15]. Therefore, developing a chaotic system/oscillator with fewer components is more interesting. Recently, chaotic oscillators using a single op-amp is more focused and considered for study [6,16–25]. Chaotic oscillators using a single op-amp based on inductor (L), capacitor (C), resistor (R) and semiconductor diode components are reported in the literature [16,17,19,26,27].

Some memristor-based chaotic oscillators with L, C components are also reported in the literature [18,21–25,28]. The available papers on the single op-amp based chaotic oscillator are categorised in Table 1.

It is noted from Table 1 that few chaotic oscillators are made of a single-opamp with resistances, capacitances and memristor. Motivated with the above-discussed literature, in this paper, a new chaotic oscillator using a single opamp, two capacitors, one resistor, one inductor, and memristive diode bridge cascaded with an inductor having a line of equilibria is proposed. In the new oscillator circuit, negative feedback, i.e. inverting terminal of the opamp is being used and the non-inverting terminal is grounded. It is to be noted that in the case of Sl. No. 9 of Table 1, (Wein-bridge oscillators) positive feedbacks and inverting terminal are used in the circuits.

Chaotic systems have been a subject of considerable interest in many areas in recent years [32–34]. Especially in recent years, a large number of studies have been conducted on random number generators (RNG). Angulo et al., performed a new oscillator-based RNG [35], avaroglu performed hardware-based RNG [35], Li et al., and Ergun and Özoguz performed real RNG [36,37], Cicek et al. performed discrete time chaos-based RNG and a new pair of entropy core RNG [38], Pareschi et al. performed high-speed RMS testing and implementation [39].

Wieczorek et al., have designed an RNG that its operating frequency is 50 MHz and bit production speed is 5 Mbit/s by using an FPGA with a double stable flip-flop, and the random numbers were subjected to statistical tests, they achieved successful results [40]. Fischer et al. performed a PLL-based oscillator using FPGA at a production rate of 1 Mbit/s and achieved successful results from NIST tests [41]. István et al. performed FPGA-based, random number generation with 50 MHz operating frequency classical jitter oscillator method and obtained successful results from NIST-800-22 tests [42].

In recent decades, many control techniques are proposed for the chaos suppression or control of the states of the chaotic system like adaptive control [43], sliding mode control (SMC) [44], backstepping control [45], contraction theory based control [46], etc. SMC is more focused among other control techniques.

In this paper, a new chaotic oscillator using a single opamp, two capacitors, one resistor, one inductor, and memristive diode bridge cascaded with an inductor having a line of equilibria is proposed. The new oscillator is analysed using the theoretical and numerical methods like Lyapunov exponents, bifurcation diagram and phase plots. Further, a non-singular terminal SMC technique is designed for the suppression of the states of the new oscillator. Finally, an application of the new oscillator is shown for the chaos based random number generation (RNG). Raspberry Pi 3 is used for the realisation of the RNG.

The remaining paper goes like this. Section 2 discusses the design of the memristor-based new chaotic oscillator containing a single op-amp L, C and R. The dynamic behaviour analyses of the proposed oscillator are discussed in Section 3. Section 4 discusses the design of a non-singular terminal SMC technique for the suppression of chaos in the states of the new oscillator. In Section 5, a random number generator is designed using the new oscillator and its randomness is tested. Finally, the conclusions of the paper are presented in Section 6.

2 Memristor-based oscillator containing a single op-amp L, C and R

In this section, the dynamics of the generalised memristor and the new system developed using the generalised memristor is discussed.

2.1 Dynamics and structure of a generalised memristor

The equivalent circuit of a generalised memristor [24,47,48] considered in this paper is shown in Figure 1. The circuit contains a diode bridge cascaded with a parallel RC filter. Voltage constraints across each pair of parallel diodes are the main cause of memristive behaviour.

In Figure 1, v_M is the voltage across the input terminal and i_M is the current flowing through the input terminal, v_o is the voltage across the capacitor and G_M is the memristor conductance. The dynamics i_M and v_o is expressed as [24,47,48] in (1).

$$\begin{cases} i_M = G_M\, v_M = 2I_s e^{-\alpha v_0} \sinh(\alpha v_M) \\ \dfrac{dv_0}{dt} = \dfrac{2I_s e^{-\alpha v_0} \cosh(\alpha v_M)}{C_0} - \dfrac{v_0}{R_0\, C_0} - \dfrac{2I_s}{C_0} \end{cases} \tag{1}$$

where $\alpha = \frac{1}{2\omega v_t}$ is a constant. The variables I_s, ω and v_t are the reverse saturation current, emission coefficient, and thermal voltage of diodes, respectively [24,47,48].

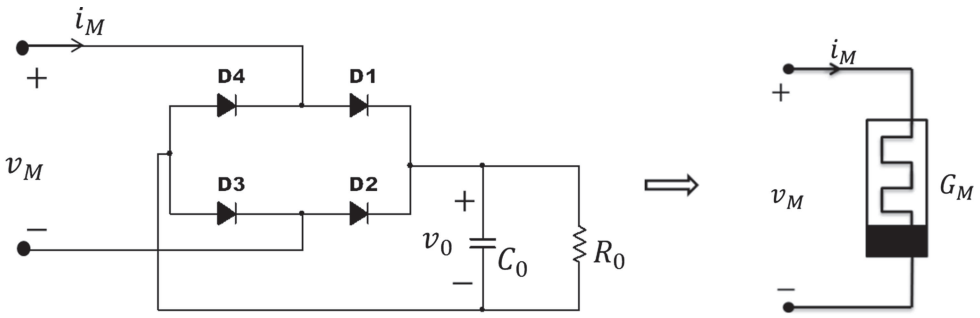

Fig. 1. A generalised memristor using a diode bridge and a parallel LC circuit [24,47,48].

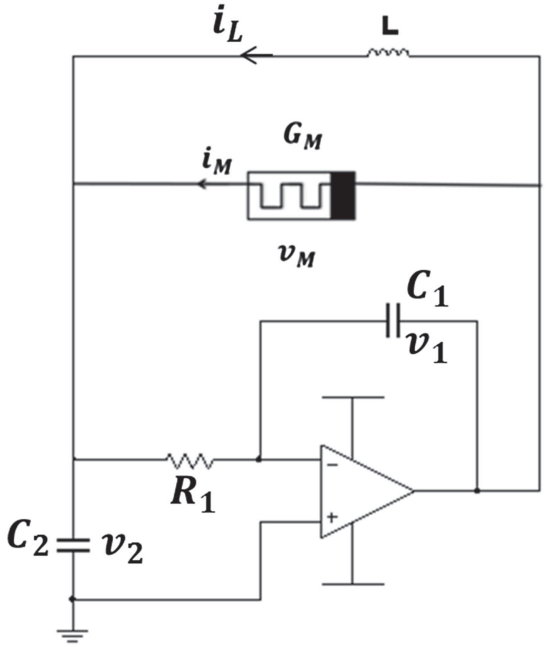

Fig. 2. The proposed oscillator containing a single op-amp, L, R, C and a generalised memristor.

The value of these parameters is $I_s = 5.84\,nA$, $\omega = 1.94$, $v_t = 0.25\,\mathrm{V}$. In Figure 1, IN1418 type of diodes is used.

2.2 New chaotic oscillator containing a single op-amp, generalised memristor L, C and R

The proposed chaotic circuit is presented in Figure 2. It is based on the generalised memristor shown in Figure 1. The circuit has a single op-amp, two capacitors C_1, C_2, an inductor L, a resistor R_1 and a memristor having a conductance G_M.

Let v_1 and v_2 be the voltage drop across capacitors C_1 and C_2, respectively, and i_L, i_M be the current flowing through the inductor and memristor, respectively, in Figure 2. Here, it is assumed that op-amp and capacitors work in their linear working range. Applying Kirchhoff's laws to the circuit in Figure 2 and using the

voltage equation for memristor given in (1), a set of four differential equations are obtained as:

$$\begin{cases} C_1 \dfrac{dv_1}{dt} = -\dfrac{v_2}{R_1} \\ C_2 \dfrac{dv_2}{dt} = -\dfrac{v_2}{R_1} + i_L + i_M \\ L \dfrac{di_L}{dt} = v_1 - v_2 \\ \dfrac{dv_0}{dt} = \dfrac{2I_s e^{-\alpha v_0} \cosh(\alpha v_M)}{C_0} - \dfrac{v_0}{C_0 R_0} - \dfrac{2I_s}{C_0} \end{cases} \tag{2}$$

Now using the expression of i_M from (1) and rearranging the terms in (2), we can write as

$$\begin{cases} \dfrac{dv_1}{dt} = \left(\dfrac{1}{C_1}\right)\left\{-\dfrac{v_2}{R_1}\right\} \\ \dfrac{dv_2}{dt} = \left(\dfrac{1}{C_2}\right)\left\{-\dfrac{v_2}{R_1} + i_l + 2I_s e^{-\alpha v_0} \sinh(\alpha v_M)\right\} \\ \dfrac{di_L}{dt} = \left(\dfrac{1}{L}\right)\{v_1 - v_2\} \\ \dfrac{dv_0}{dt} = \left(\dfrac{1}{C_0}\right)\left\{2I_s e^{-\alpha v_0} \cosh(\alpha v_M) - \dfrac{v_0}{R_0} - 2I_s\right\} \end{cases} \tag{3}$$

We consider the following new variables for a change of variables and parameters

$$\begin{cases} \sigma = \sqrt{\frac{L}{C_2}},\ x_1 = v_1, x_2 = v_2,\ x_3 = i_L\sigma,\ a = \frac{\sigma}{R},\ b = \frac{C_2}{C_1},\ t = \tau\sqrt{L\,(C_2)}, \\ c = \frac{\sqrt{L(C_2)}}{C_0},\ v_M = x_1 - x_2 \end{cases} \tag{4}$$

The normalised dimensionless circuit equations are expressed in (5).

$$\begin{cases} \dot{x}_1 = -abx_2 \\ \dot{x}_2 = -ax_2 + x_3 + 2I_s\sigma e^{-\alpha(x_4)} \sinh(\alpha(x_1 - x_2)) \\ \dot{x}_3 = x_1 - x_2 \\ \dot{x}_4 = c\{2I_s e^{-\alpha(x_4)} \cosh(\alpha(x_1 - x_2)) - \frac{1}{R_0}(x_4) - 2I_s\} \end{cases} \tag{5}$$

The system in (5) has four nonlinear terms including two exponential terms, one cosine hyperbolic and sine hyperbolic.

The system in (5) has an asymmetry to its axes, planes and spaces and is not invariant under the coordinate transformations.

The equilibrium point of the system in (5) is obtained as $E = \Big(0, 0, 0, e^{-\alpha(x_4)} - \frac{1}{2I_s R_0}(x_4) = 1\Big)$. The only value of (x_4) which satisfies the condition of E is zero. Hence, the equilibrium point of the system in (5) is the origin.

The system in (5) has chaotic behaviour for the set of parameters $a = 120$, $b = 2.52, c = 310.62$, $\alpha = 10.309$, $\sigma = 316.62, R_0 = 20$, $I_s = 3.048 \times 10^{-9}$. The Lyapunov exponents for the above set of parameters are calculated by using the Wolf et al. algorithm [49] and found as $L_i = (0.9012, 0, -6.383, -13.4639)$. The presence of one positive Lyapunov exponents reflects that the system has chaotic behaviour. Chaotic attractors of System (5) with the above set of parameters and $x(0) = (0.01, 0.014, 0.05, 0.01)^T$ are shown in Figure 3.

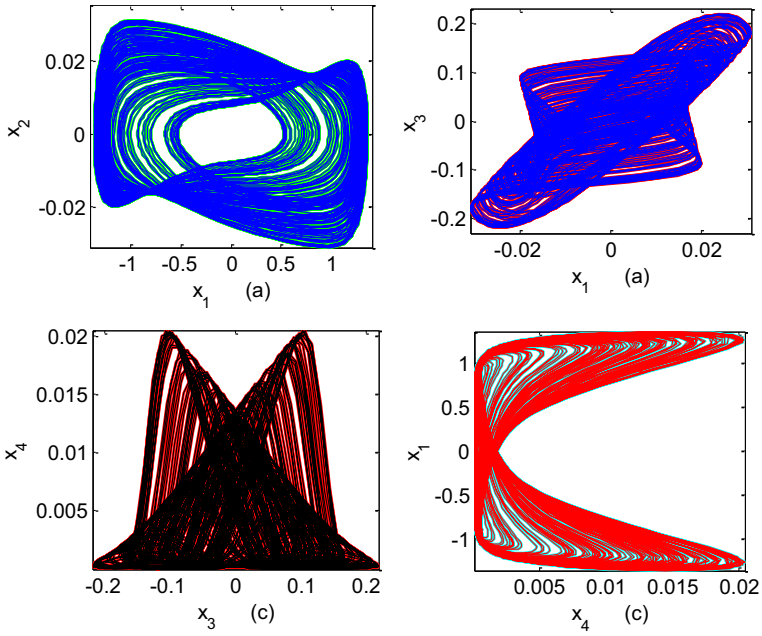

Fig. 3. Chaotic attractors of System (5).

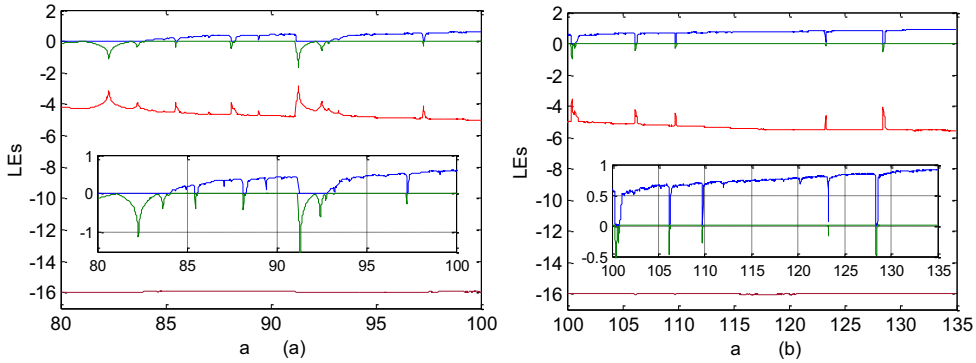

Fig. 4. Lyapunov spectrum with the variation of parameter a and $b = 2.52$, $c = 310.62$, $\alpha = 10.309$, $\sigma = 316.62$, $R_0 = 20$, $I_s = 3.048 \times 10^{-9}$.

3 Dynamic behaviours of the proposed system in (5)

Dynamic behaviours of System (5) are investigated using the bifurcation diagram and Lyapunov spectrum plots. All these plots are obtained by varying one parameter at a time and keeping the other parameters fixed. Lyapunov spectrum is obtained by finding the Lyapunov exponents with fixed initial conditions $x(0) = (0.01, 0.014, 0.05, 0.01)^T$. Lyapunov spectra with the variation of parameters a and b are shown in Figures 4 and 6, respectively. Bifurcation diagram plots using the continuation method, and with the variation of parameters a and b are shown in Figures 5 and 7, respectively. Lyapunov spectrum plots and bifurcation diagrams with the variation of parameter c are not shown here, because in this case, the

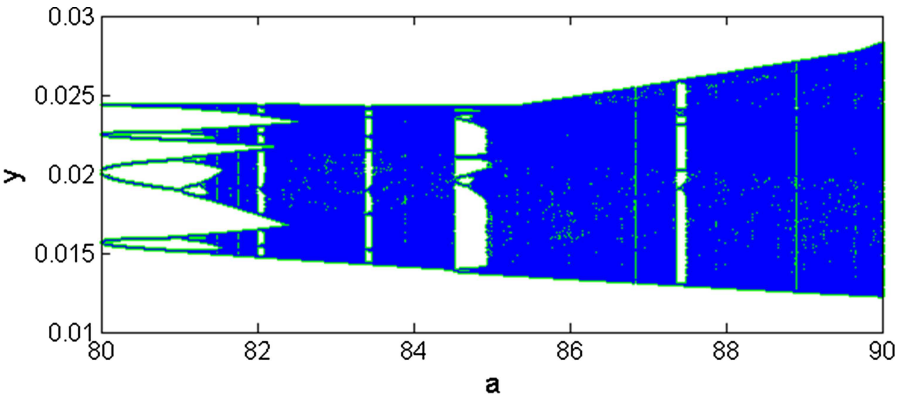

Fig. 5. Bifurcation diagram using the continuation method, and by varying parameter a with $b = 2.52$, $c = 310.62$, $\alpha = 10.309$, $\sigma = 316.62, R_0 = 20$, $I_s = 3.048 \times 10^{-9}$.

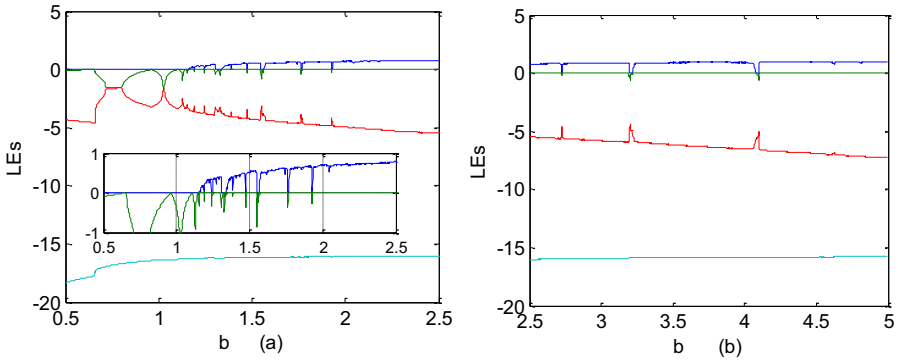

Fig. 6. Lyapunov spectrum by varying parameter b with $a = 120$, $c = 310.62$, $\alpha = 10.309$, $\sigma = 316.62, R_0 = 20$, $I_s = 3.048 \times 10^{-9}$.

dynamical behaviours of the system are same. Thus, to avoid the repetition and to restrict the length of the paper, the results with the variation of parameter c are not shown here. It is apparent from the Figure 5 that in case of the bifurcation diagram using continuation method there is a change in behaviour of the system for parameter a in the ranges: $81.3 < a < 84.0$, where the system has chaotic behaviour; for the region $84.51 < a < 84.71$ and $87.35 < a < 87.75$, the system has periodic behaviour; for the region $0.34 < b < 1$, the system has chaotic behaviour.

Coexistence of chaotic attractors with $a = 120$, $b = 2.52$, $c = 310.62$, $\alpha = 10.309$, $\sigma = 316.62, R_0 = 20$, $I_s = 3.048 \times 10^{-9}$ and $x(0) = (\pm 1.001,\ 0.0014,\ 0.005, \pm 10.5101)^T$ are shown in Figure 8.

4 Design of non-singular terminal SMC technique for the regulation of the states

In this section, a non-singular terminal SMC technique is designed for the suppression of chaos in the states of the new oscillator. The system dynamics (5) is rewritten with control input in (6).

$$\begin{cases} \dot{x}_1 = -abx_2 \\ \dot{x}_2 = -ax_2 + x_3 + 2I_s\sigma e^{-\alpha(x_4)} \sinh(\alpha(x_1 - x_2)) + u_1 \\ \dot{x}_3 = x_1 - x_2 + u_2 \\ \dot{x}_4 = c\{2I_s e^{-\alpha(x_4)} \cosh(\alpha(x_1 - x_2)) - \frac{1}{R_0}(x_4) - 2I_s\} + u_3 \end{cases} \tag{6}$$

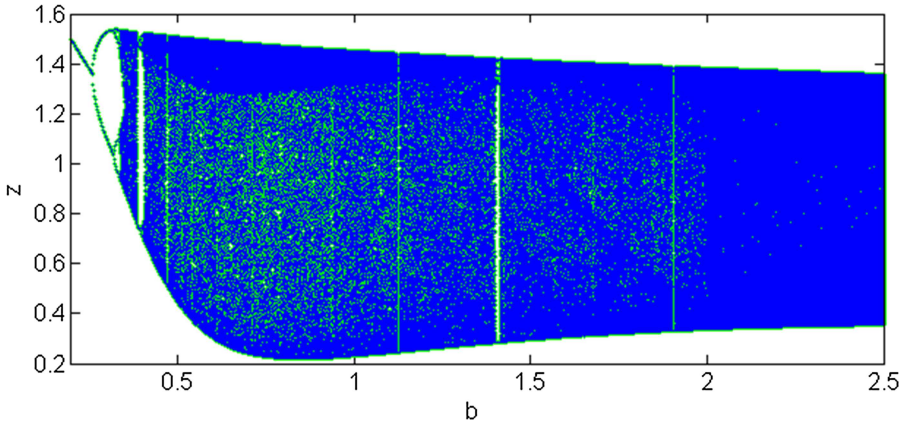

Fig. 7. Bifurcation diagram using the continuation method, and by varying parameter b with $a = 120$, $c = 310.62$, $\alpha = 10.309$, $\sigma = 316.62$, $R_0 = 20$, $I_s = 3.048 \times 10^{-9}$.

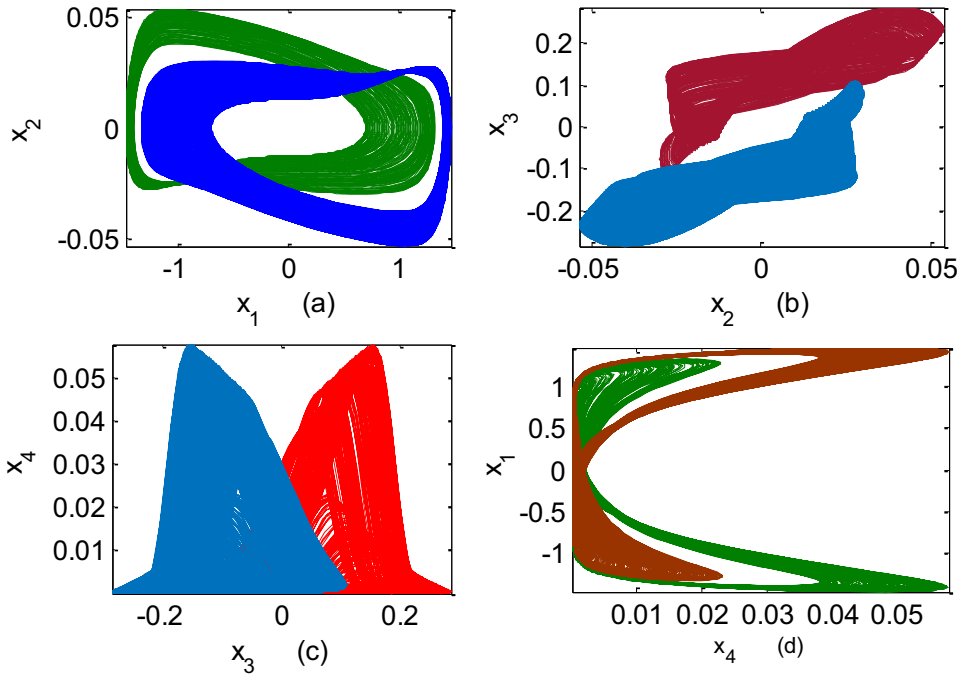

Fig. 8. Coexistence of chaotic attractors with $a = 100$, $b = 2.52$, $c = 310.62$, $\alpha = 10.309$, $\sigma = 316.62$, $R_0 = 20$, $I_s = 3.048 \times 10^{-9}$.

where u_1, u_2, u_3 are the added control inputs. The expressions of these control inputs are obtained by designing of a non-singular terminal SMC. For the above plant, the control inputs u1 and u2 are so designed such that the above system can be represented in a strict feedback form,

$$u1 = ax_2 - x_3 - 2I_s\sigma e^{-\alpha(x_4)}\sinh(\alpha(x_1 - x_2)) - \frac{x_3}{ab}$$
$$u2 = x_4 - x_1 + x_2 \tag{7}$$

Using u1 and u2, the above system in (6) is written as,

$$\begin{aligned}\dot{x}_1 &= -abx_2\\ \dot{x}_2 &= -\frac{x_3}{ab}\\ \dot{x}_3 &= x_4\\ \dot{x}_4 &= c\{2I_s e^{-\alpha(x_4)}\cosh(\alpha(x_1-x_2)) - \frac{1}{R_0}(x_4) - 2I_s\} + u3\end{aligned} \tag{8}$$

Now, u3 is designed using a non-singular terminal sliding mode such that the above system in (8) gets stabilised. A transformation is used for representing (8) as a chain of integrators.

$$\begin{aligned}\dot{z}_1 &= z_2\\ \dot{z}_2 &= z_3\\ \dot{z}_3 &= z_4\\ \dot{z}_4 &= f(z) + u3\end{aligned} \tag{9}$$

where, $z_1 = x_1$, $z_2 = -abx_2$, $z_3 = x_3$, $z_4 = x_4$, and

$$f(z) = c\left\{2I_s e^{-\alpha(z_4)}\cosh\left(\alpha\left(z_1 + \frac{z_2}{ab}\right)\right) - \frac{1}{R_0}(z_4) - 2I_s\right\} \tag{10}$$

Now the sliding surface is chosen as

$$\mathrm{S} = z_4 + 6\,|z_3|^{\alpha_3}\,\mathrm{sign}(z_3) + 11\,|z_2|^{\alpha_2}\,\mathrm{sign}\,(z_2) + 6\,|z_1|^{\alpha_1}\,\mathrm{sign}(z_1) \tag{11}$$

where the constant α_i is chosen as

$$\alpha_{i-1} = \frac{\alpha_i \alpha_{i+1}}{2\alpha_{i+1} - \alpha_i} \tag{12}$$

such that $\alpha_n = 1$, where n is the total number of states. For our case $\alpha_1 = \frac{2}{5}$, $\alpha_2 = \frac{1}{2}$, $\alpha_3 = \frac{2}{3}$. Now, a saturation function $\mathrm{sat}(u_f, u_s)$ is chosen so that the singularities in terminal sliding mode can be avoided as explained in [50] where,

$$u_f = -6\alpha_3\,|z_3|^{\alpha_3 - 1}\,\mathrm{sign}(z_3) - 11\alpha_2\,|z_2|^{\alpha_2 - 1}\,\mathrm{sign}(z_2) - 6\alpha_1\,|z_1|^{\alpha_1 - 1}\,\mathrm{sign}(z_1) \tag{13}$$

The control law u_3 is given in (14).

$$u_3 = -f(z) + \mathrm{sat}(u_f, u_s) - \mathrm{ksign}(s) \tag{14}$$

Using the control inputs u_1, u_2, u_3 given in (7) and (14), the states x_1, x_2, x_3 and x_4 converges to zero as $t \to \infty$.

The simulation results for the suppression of chaos in the states are given in Figure 9. Here, the initial conditions considered for the states are $x(0) = (0.01, 0.015, 0.05, 0.01)^T$. It is apparent from Figure 9 that all the states are regulated to their desired value, i.e. the zero.

5 Random number generator design and its randomness tests using the system in (5)

In this section, chaos-based random number generator is designed. Random number generators (RNGs) are used in all kinds of scientific and engineering areas where

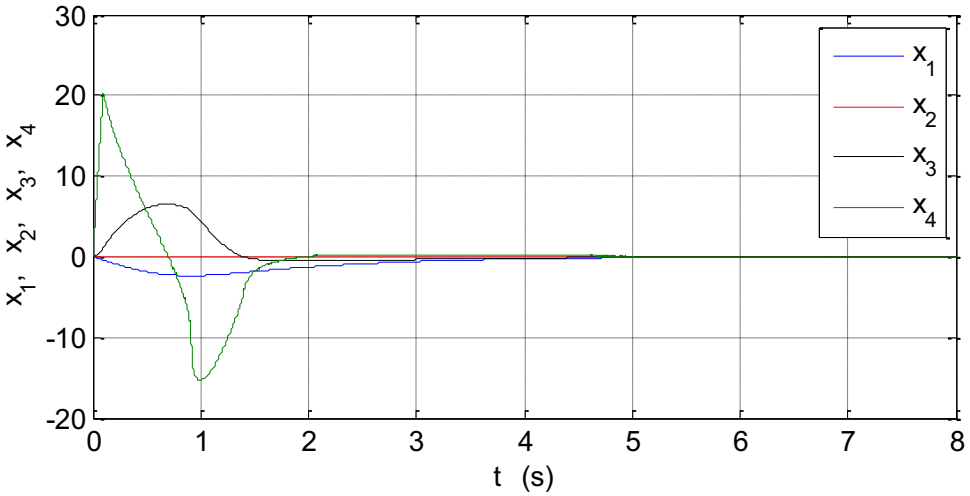

Fig. 9. Stabilisation of states of System (5).

Table 2. RNG algorithm pseudo code.

Algorithm: Random Number Generation Algorithm Pseudo code
Input: Parameters and initial condition of chaotic systems
Output: Ready tested random numbers
1: START Entering system parameters and initial conditions of a 4D chaotic system
2: Determination of the value of Δh (0.005)
3: Sampling with determination Δh value for RK4
4: WHILE (minimum 1MBit data) **DO**
5: Solving the 4D chaotic system using RK4 algorithm
6: Obtaining time series as float numbers (x, y, z and w)
7: Convert float to 32-bit binary numbers
8: Select LSB-16 bits from RNG from x, y, z and w phases
9: END WHILE
10: Apply NIST-800-22 Tests for each minimum 1MBit data
11: IF (test results == pass) **THEN**
12: Ready tested random numbers for RNG applications
13: ELSE (test results == false)
14: Go to step 4
15: END IF
16: END
17: EXIT

random number sequences, especially cryptology, are required [51]. In this study, the design of the RNG is made by using (5). For the design, the continuous-time chaotic system is discretised by RK4 numerical solution method by entering certain step intervals. Then the discretised chaotic system is converted to 32-bit binary number format. Then, for all outputs (x, y, z, w), the 16 least significant bits (LSB) are taken and a random number sequence is created. The pseudo code for the design of the RNG is given as follows.

Internationally accepted NIST-800-22 tests are used for the success of random numbers. The NIST-800-22 test consists of 16 different tests and requires at least 1 Mbit data set. The success of these 16 tests is required for randomness success.

Table 3. NIST-800-22 test results of random numbers obtained from x, y, z and w.

Statistical tests	P-value (x_16bit)	P-value (y_16bit)	P-value (z_16bit)	P-value (w_16bit)	Result
Frequency (Monobit) test	0.6686	0.3134	0.5605	0.1675	Successful
Block-frequency test	0.4794	0.8777	0.9178	0.4591	Successful
Cumulative-sums test	0.7233	0.5648	0.7111	0.3259	Successful
Runs test	0.7247	0.2289	0.4558	0.6773	Successful
Longest-run Test	0.1900	0.7454	0.5633	0.0763	Successful
Binary matrix rank test	0.2873	0.7305	0.2849	0.8612	Successful
Discrete fourier transform test	0.5206	0.3216	0.1803	0.7550	Successful
Non-overlapping templates test	0.2423	0.5079	0.1977	0.2803	Successful
Overlapping templates test	0.1550	0.4637	0.2338	0.6679	Successful
Maurer's universal statistical test	0.3404	0.6027	0.7499	0.8513	Successful
Approximate entropy test	0.6236	0.6895	0.5011	0.9533	Successful
Random-excursions test ($x = -4$)	0.5583	0.3601	0.8436	0.6578	Successful
Random-excursions variant test ($x = -9$)	0.6281	0.8062	0.5511	0.4513	Successful
Serial test-1	0.9903	0.9685	0.1950	0.1305	Successful
Serial test-2	0.9814	0.9953	0.4827	0.0550	Successful
Linear-complexity test	0.3454	0.1881	0.4426	0.8894	Successful

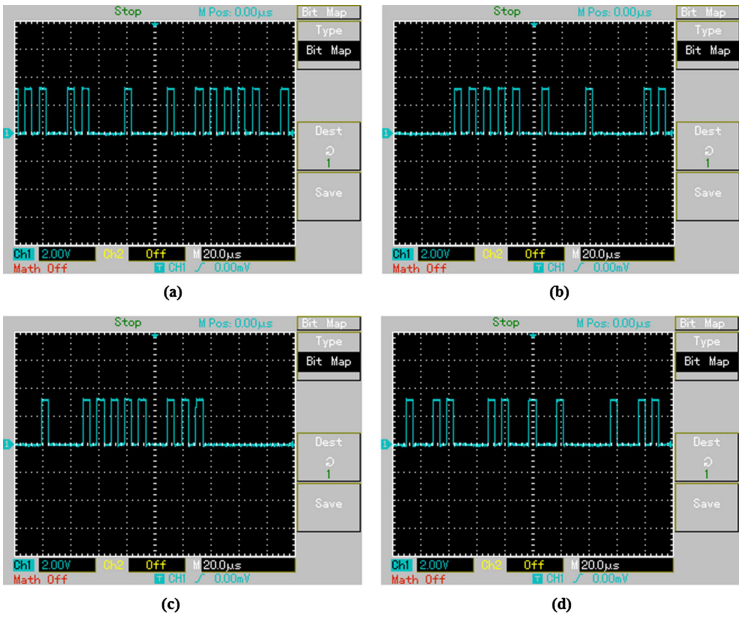

Fig. 10. Oscilloscope images of random numbers from x (a), y (b), z (c), w (d) outputs.

The results of the 16 different tests are evaluated by paying attention to the P value. For the test to be successful, the P value should be greater than 0.001 [51]. If the test results are not obtained successfully, the loop is continued by altering the LSB bits and the pitch interval. Using the LSB 16 bits from each dimension of the 4-dimensional system used in this study, random number generation is performed, and each passes the NIST-800-22 tests successfully. The results of the NIST-800-22 test P values of each dimension are shown in Table 3.

Raspberry Pi 3 is used for the realisation of the RNG. The Raspberry Pi outputs of the random numbers generated from the chaotic system, i.e. the oscilloscope screen outputs shown in Figure 10.

6 Conclusions

This paper reports a new chaotic oscillator using a single op-amp, two capacitors, one resistor, one inductor, and memristive diode bridge cascaded with an inductor. The new oscillator has a line of equilibria. In the new oscillator circuit, negative feedback is used. The new oscillator based on the memristive diode bridge is different from the available similar systems. The new oscillator depicts chaotic, periodic, quasi-periodic behaviour. Lyapunov spectrum plot, bifurcation diagram, phase plot, etc. are used to analyse the new oscillator. Further, a non-singular terminal sliding mode control (N-TSMC) is designed for the suppression of chaos in the states of the new oscillator. Moreover, an application of the new oscillator is shown by designing a chaos-based random number generator. Raspberry Pi 3 is used for the realisation of the random number generator.

The authors gratefully acknowledge the anonymous reviewers for their valuable comments and suggestions that have helped to improve the standard of the manuscript.

Author contribution statement

All authors have made significant technical contributions to the paper and share responsibility and accountability for the results.

References

1. M. Di Ventra, Y.V. Pershin, L.O. Chua, Proc. IEEE **97**, 1717 (2009)
2. A.L. Fitch, H.H.C. Lu, D.S. Yu, Chaos in a memcapacitor based circuit, in *2014 IEEE Int. Symp. Circuits Syst.* (Melbourne VIC, Australia, 2014), pp. 482–485
3. L.O. Chua, IEEE Trans. Circuit Theory. **18**, 507 (1971)
4. D.B. Strukov, G.S. Snider, D.R. Stewart, R.S. Williams, Nature **453**, 80 (2008)
5. M. Itoh, L.O. Chua, Int. J. Bifurc. Chaos. **18**, 3183 (2008)
6. F.Y. Recai Kilic, Chaos Solitons Fractals **38**, 1394 (2008)
7. A. Bussarino, L. Fortuna, M. Franca, L.V. Gambuzza, Int. J. Bifurc. Chaos. **23**, 1330015 (2013)
8. A.L. Fitch, D. Yu, H.H.C. Iu, V. Sreeram, Int. J. Bifurc. Chaos. **22**, 1250133 (2012)
9. A. Buscarino, L. Fortuna, M. Frasca, L. Valentina Gambuzza, Chaos **22**, 023136 (2012)
10. F. Corinto, A. Ascoli, M. Gilli, IEEE Trans. Circuits Syst. I Regul. Pap. **58**, 1323 (2011)
11. B. Bao, Z. Ma, J. Xu, Z. Liu, Q. Xu, Int. J. Bifurc. Chaos. **21**, 2629 (2011)
12. M. Itoh, L.O. Chua, Int. J. Bifurc. Chaos. **18**, 3183 (2008)
13. B.C. Bao, J.P. Xu, G.H. Zhou, Z.H. Ma, L. Zou, Chin. Phys. B. **20**, 120502 (2011)
14. X. Han, H. Wu, B. Fang, Neurocomputing. **201**, 40 (2016)
15. J.C. Sprott, Int. J. Bifurc. Chaos. **21**, 2391 (2011)
16. T. Banerjee, B. Karmakar, B.C. Sarkar, Nonlinear Dyn. **62**, 859 (2010)
17. T. Banerjee, B. Karmakar, B.C. Sarkar, AEU - Int. J. Electron. Commun. **66**, 593 (2012)
18. B. Bao, T. Jiang, Q. Xu, M. Chen, H. Wu, Y. Hu, Nonlinear Dyn. **86**, 1711 (2016)
19. T. Banerjee, B. Karmakar, D. Biswas, B.C. Sarkar, A simple inductor-free autonomous chaotic circuit, in *MDCCT-2012* (Burdwan University, India, 2012)

20. X.-S. Yang, Q. Li, Electron. Lett. **38**, 623 (2002)
21. H. Bao, N. Wang, H. Wu, Z. Song, B. Bao, IETE Tech. Rev. **36**, 109 (2018)
22. X. Ye, J. Mou, C. Luo, Z. Wang, Nonlinear Dyn. **92**, 923 (2018)
23. H. Wu, B. Bao, Z. Liu, Q. Xu, P. Jiang, Nonlinear Dyn. **83**, 893 (2015)
24. N. Wang, B. Bao, T. Jiang, M. Chen, Q. Xu, Math. Prob. Eng. **2017**, 29 (2017)
25. M. Taher, Z.J. Khalifa, Int. J. Electr. Eng. Educ. **53**, 280 (2016)
26. W. San-Um, B. Suksiri, P. Ketthong, Int. J. Bifurc. Chaos. **24**, 1450155 (2014)
27. J. Kengne, N. Tsafack, L.K. Kengne, Int. J. Dyn. Control. **6**, 1543 (2018)
28. B.C. Bao, P.Y. Wu, H. Bao, H.G. Wu, X. Zhang, M. Chen, Chaos Solitons Fractals **109**, 146 (2018)
29. A.S. Elwakil, M.P. Kenned, J. Franklin Inst. **336**, 687 (1999)
30. T. Banerjee, Nonlinear Dyn. **68** 565 (2012)
31. Q. Xu, Q. Zhang, T. Jiang, B. Bao, M. Chen, Circuit World. **44**, 108 (2018)
32. S. Çiçek, A. Feriko lua, I. Pehlivan, Optik (Stuttg). **127**, 4024 (2016)
33. J.P. Singh, K. Lochan, N.V. Kuznetsov, B.K. Roy, Nonlinear Dyn. **90**, 1277 (2017)
34. J.P. Singh, B.K. Roy, Nonlinear Dyn. **93**, 1121 (2018)
35. J. Angulo, E. Kussenar, H. Barthelemy, B. Duval, A new oscillator-based RNG, in *IEEE Faibl. Tens. Faibl. Cons.* (2012), pp. 1–4
36. S. Ergün, S. Özoğuz, Int. J. Electron. Commun. **61**, 235 (2007)
37. Q. Li, Q. Liu, J. Niu, Chaotic oscillator with potentials in TRNG and ADC, in *35th Int. Conf. Telecomm. Signal Proc.* (2012), pp. 397–400
38. I. Cicek, A. Pusane, G. Dundar, Integr. VLSI J. **47**, 38 (2014)
39. F. Pareschi, G. Setti, R. Rovatti, IEEE Trans. Circuits Syst. **57**, 3124 (2010)
40. P. Wieczorek, K. Golofit, IEEE Trans. Circuits Syst. **61**, 134 (2014)
41. V. Fischer, M. Drutavosky, M. Simka, N. Bochard, High performance TRNG in sltera stratix FPLDs, in *F. Program. Log. App.* (2004), pp. 555–564.
42. H. Istvan, A. Suciu, O. Cret, FPGA based TRNG using automatic calibratio, in *Intell. Comp. Comm. Proc. IEEE 5th Int. Conf. ICCP* (2009), pp. 373–376
43. C. Hu, J. Yu, Chaos Solitons Fractals **91**, 262 (2016)
44. J.P. Singh, B.K. Roy, Trans. Inst. Meas. Control **40**, 3573 (2017)
45. H. Yu, J. Wang, B. Deng, X. Wei, Y. Che, Y.K. Wong, W.L. Chan, K.M. Tsang, Commun. Nonlinear Sci. Numer. Simul. **17**, 1344 (2012)
46. J.P. Singh, B.K. Roy, Nonlinear Dyn. **92**, 23 (2018)
47. F. Corinto, A. Ascoli, Electron. Lett. **48**, 824 (2012)
48. B. Bao, J. Yu, F. Hu, Z. Liu, Int. J. Bifurc. Chaos. **24**, 1450143 (2014)
49. A. Wolf, J.B. Swift, H.L. Swinney, J.A. Vastano, Physica D **16**, 285 (1985)
50. Y. Feng, X. Yu, F. Han, Automatica **49**, 1715 (2013)
51. E. Avaroglu, M. Turk, RNG using multi-mode chaotic attractor, in *IEEE Signal Process. Comm. Appl. Conf.* (2013)